arXiv:nucl-th/0403022v1 8 Mar 2004

On the usefulness of the spectral function concept

J. Golak, H. Witała, R. Skibiński

M. Smoluchowski Institute of Physics,

Jagiellonian University, PL-30059 Kraków, Poland

W. Glöckle

Institut für Theoretische Physik II,

Ruhr Universität Bochum, D-44780 Bochum, Germany

A. Nogga

Institute for Nuclear Theory, University of Washington,

Box 351550 Seattle, WA 98195, USA

H. Kamada

Department of Physics, Faculty of Engineering,

Kyushu Institute of Technology, 1-1 Sensuicho,

Tobata, Kitakyushu 804-8550, Japan

(Dated: February 8, 2008)

Abstract

The usefulness of the spectral function S in the process $^3\mathrm{He}(e,e'N)$ has been investigated in a kinematical regime constrained by the conditions that the three-nucleon (3N) center-of-mass energy $E_{3N}^{c.m.} \leq 150$ MeV and the magnitude of the three-momentum transfer, $\mid \vec{Q} \mid \leq 600$ MeV/c. Results based on a full treatment of the final state interaction are compared to the spectral function approximation. In the case of proton knockout in the direction of the photon kinematical conditions have been identified where both response functions, R_L and R_T, can be well approximated by S. These conditions occur for certain low missing momenta and missing energies but not in all cases. So care is required. In case of neutron knockout only R_T is a candidate for an approximate treatment by S. In the case of R_L the concept of using S is not valid in the studied kinematical regime. This does not exclude the possibility that beyond that regime it might be useful. Possible applications using S for the extraction of electromagnetic form factors of the nucleons are pointed out.

PACS numbers: 21.45+v,21.10-k,25.10+s,25.20-x

I. INTRODUCTION

The $(e, e'N)$ reactions have been widely analyzed in the past using the concept of the spectral function. This quantity has been introduced for instance in the work of [1, 2] in the context of inclusive electron scattering on ^{3}He. In the following it has been intensively investigated by C. Ciofi degli Atti and collaborators [3, 4, 5, 6, 7] and P.U. Sauer and collaborators [8, 9, 10] as well as other groups. For heavier systems there is a rich literature where that tool has been also extensively used [11]. More recent work can be found in [12] and [13, 14]. In [12] effects of polarizations are included. In no case the full final state interaction (FSI) has been dealt with.

The concept of the spectral function in $(e, e'N)$ reactions is based on the simplifying assumption that the nucleon is knocked out as a free particle and only the remaining nucleons interact among themselves. Thus for a ^{3}He target only a final state interaction between two nucleons is considered. Also the antisymmetrization of the knocked out nucleon with the other two nucleons is neglected. This picture appears to be reasonable if the knocked out nucleon receives all or essentially all of the photon three-momentum, which moreover should be not too small. Of course that simplification was also enforced in the past by the simple fact that the complete final state interaction could not be controlled numerically.

Integrating over a certain missing energy interval one defines "momentum distributions". We put that quantity into quotes since it is not the true momentum distribution inside for instance ^{3}He. The reason is the restricted integration interval even if the approximation underlying the use of the spectral function would be justified.

Over the years it has become possible to take FSI among the three nucleons completely into account in the case of ^{3}He [15]. We present such a solution and critically investigate the simplified picture leading to the spectral function. Our framework, however, is still non-relativistic, which forces us to stay below the pion threshold, thus below about 150 MeV 3N c.m. energy. In order not to induce too high nucleon momenta, which also would require a relativistic treatment, we restricted the three-momenta of the photon to the maximally allowed values of 600 MeV/c. Though this is already a too high value, we used it to get a first indication whether there will be a tendency that at the higher momenta the final state interaction might decrease. Also we expect that this violation will not be too severe to prevent a reasonable insight into the failure or validity of the assumptions underlying the

simplistic picture of the spectral function.

The paper is organized as follows. Section II is a brief reminder of the definition of the spectral function and of the complete formulation for the final state interaction in case of ^{3}He. The two relevant pairs of kinematical variables for $(e, e'N)$ processes are the missing momentum and missing energy, k and E, and the virtual photon momentum and its energy, Q and ω. So in Sec. II we also illustrate the mappings of the two related regions in the $k-E$ and $Q-\omega$ planes. In Sec. III we compare the spectral function under various kinematical conditions to results taking the full final state interaction into account. This investigation is performed for proton and neutron knockout from ^{3}He. We summarize in Sec. IV.

II. THEORETICAL FRAMEWORK

We regard the semi-exclusive process $^3\mathrm{He}(e, e'N)$ in parallel kinematics, where the nucleon N is knocked out with the momentum $\vec{p}_1$ parallel to the virtual photon momentum $\vec{Q}$. In the unpolarized case the cross section is simply given as

$$\frac{d^6\sigma}{dE_{e'}d\Omega_{e'}d\Omega_1 dE_1} = \sigma_{\mathrm{Mott}} \int d\hat{p}\ [v_L R_L + v_T R_T]\ \frac{m^2\, p\, p_1}{2}, \tag{1}$$

since the response functions R_{TT} and R_{TL} vanish under the parallel condition [16, 17]. The functions v_L and v_T are standard kinematical factors. The two response functions R_L and R_T are expressed in terms of the nuclear matrix elements N_0 and $N_{\pm 1}$ as

$$\begin{aligned} R_L &\equiv \frac{1}{2}\sum_M \sum_{m_1,m_2,m_3} \left|N_0(\vec{p}_1,\vec{p}_2,\vec{p}_3; M, m_1, m_2, m_3; \nu_1,\nu_2,\nu_3)\right|^2, \\ R_T &\equiv \frac{1}{2}\sum_M \sum_{m_1,m_2,m_3} \Big(\left|N_1(\vec{p}_1,\vec{p}_2,\vec{p}_3; M, m_1, m_2, m_3; \nu_1,\nu_2,\nu_3)\right|^2 \\ &\qquad + \left|N_{-1}(\vec{p}_1,\vec{p}_2,\vec{p}_3; M, m_1, m_2, m_3; \nu_1,\nu_2,\nu_3)\right|^2\Big), \end{aligned} \tag{2}$$

where M, m_1, m_2, m_3 are the initial ^{3}He and final 3N spin magnetic quantum numbers, and ν_1, ν_2, ν_3 are isospin magnetic quantum numbers needed to identify the nucleons in the final state. The direction (magnitude) of the relative momentum of the two undetected nucleons is denoted by $\hat{p}$ (p) and the nucleon mass by m. The matrix elements N_0 and $N_{\pm 1}$ are driven by the charge density operator and spherical components of the transverse current operator,

respectively. In general the nuclear matrix element has the form

$$N^\mu \equiv \langle \Psi_f^{(-)} \mid j^\mu(\vec{Q}) \mid \Psi_{^3\mathrm{He}} \rangle, \tag{3}$$

where f comprises the momenta and the magnetic spin and isospin quantum numbers of the three final nucleons. We shall concentrate here on the complete break up and refer the reader for the case of the pd breakup to [18]. As has been shown in [18], N^μ can be represented as

$$N^\mu = \langle \phi_0 \mid (1+P) j^\mu(\vec{Q}) \mid \Psi_{^3\mathrm{He}} \rangle \; + \; \langle \phi_0 \mid (1+P) \mid U^\mu \rangle, \tag{4}$$

where the auxiliary state $\mid U^\mu \rangle$ obeys the Faddeev-like integral equation

$$\mid U^\mu \rangle \; = \; tG_0(1+P) j^\mu(\vec{Q}) \mid \Psi_{^3\mathrm{He}} \rangle \; + \; tG_0 P \mid U^\mu \rangle. \tag{5}$$

The ingredients in Eq. (5) are the free 3N propagator G_0, the NN t-operator generated via the Lippmann-Schwinger equation from any modern NN interaction, and a suitably chosen permutation operator P [19]. The state ϕ_0 in Eq. (4) is a plane wave, antisymmetrized in the two-body subsystem, where t acts. For a generalization including a three-nucleon force we refer the reader to [18]. In the present study we restrict ourselves to NN forces and allow only for one-body currents $j_\mu(\vec{Q})$. It is illustrative to present the physical content of the expressions (4) and (5) in the following way. If one iterates the integral equation and inserts the resulting terms into (4) one arrives at the infinite sequence of processes shown in Fig. 1. In the first row there is no final state interaction and the photon is absorbed by nucleons 1, 2 and 3. The next three rows include rescattering processes of first order in the NN t-operator (denoted by a circle). Then follow processes of second order in t, third order etc. That complete sum of processes is generated by solving the integral equation (5). Now taking only the first diagrams in row 1 and 2 into account underlies the concept of the spectral function S. The corresponding expression is

$$N^\mu = \langle \phi_0 \mid (1 + t_{23} G_0) j^\mu(\vec{Q}; 1) \mid \Psi_{^3\mathrm{He}} \rangle, \tag{6}$$

where the argument 1 in the current explicitly indicates that the photon is absorbed only on one nucleon, numbered 1 in our notation. That approximation, the two encircled diagrams

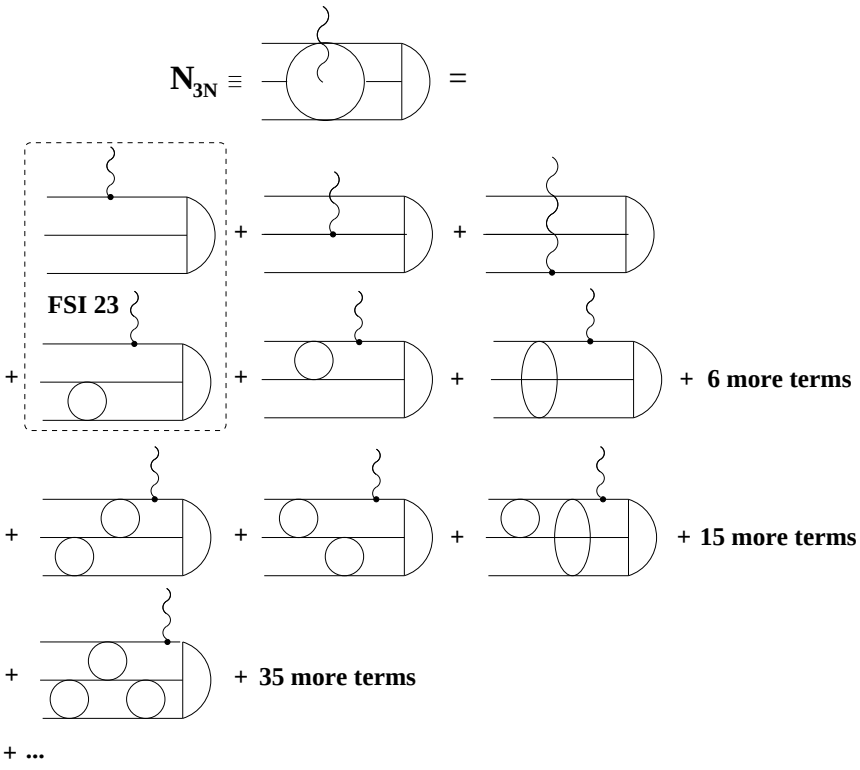

FIG. 1: Diagrammatic representation of the nuclear matrix element for the three-body electrodisintegration of ^{3}He. The open circles and ovals represent the two-body t-matrices. Three horizontal lines between photon absorption and forces, and between forces describe free propagation. The half-moon symbol on the very right stands for ^{3}He.

in Fig. 1, will be called in the following FSI23 for short and stands for final state interaction in the spectator pair (23). Related to that nuclear matrix element is the spectral function S. It is defined as

$$S(k,E) = \frac{m\,p}{2}\,\frac{1}{2}\sum_{M}\sum_{m_1,m_2,m_3}\int d\hat{p}\,\left|\sqrt{6}\,\langle\nu_1\nu_2\nu_3 \mid \langle m_1 m_2 m_3 \mid \langle\vec{p}\,\vec{k} \mid (1+t_{23}G_0) \mid \Psi_{^3\mathrm{He}}\rangle\right|^2 \quad (7)$$

The arguments of S are the magnitude k of the missing momentum

$$k \equiv \mid \vec{Q} - \vec{p}_1 \mid \quad (8)$$

and the excitation energy E of the undetected pair. Nonrelativistically

$$E \equiv \frac{p^2}{m}, \quad (9)$$

where p is the relative momentum of the undetected nucleons. Comparing the expression (7) for S to the ones for R_L and R_T under the FSI23 approximation one finds

$$\begin{aligned} S(k,E) &= \frac{1}{2}\, m\, p\, \frac{1}{(G_E)^2} \int d\hat{p} R_L(FSI23) \\ &= \frac{1}{2}\, m\, p\, \frac{2m^2}{Q^2 (G_M)^2} \int d\hat{p} R_T(FSI23). \end{aligned} \tag{10}$$

This inserted into (1) yields the well known relation between the cross section and the spectral function

$$\frac{d^6\sigma}{dE_{e'} d\Omega_{e'} d\Omega_1 dd E_1} = \sigma_{\rm Mott} \left[v_L (G_E)^2 + v_T \frac{Q^2 (G_M)^2}{2m^2} \right] S(k,E)\, m\, p_1 \;\equiv\; \sigma_{eN}\, S(k,E)\, \rho_f. \tag{11}$$

Here the non-relativistic phase space factor ρ_f is simply

$$\rho_f = m\, p_1 \left(1 + \frac{2E_e}{m} \sin^2 \frac{\theta_e}{2} \right) \tag{12}$$

and the unpolarized electron-nucleon cross section in the non-relativistic approximation reads

$$\sigma_{eN} = \sigma_{\rm Mott} \left[v_L (G_E)^2 + v_T \frac{Q^2 (G_M)^2}{2m^2} \right] \frac{1}{1 + \frac{2E_e}{m} \sin^2 \frac{\theta_e}{2}} \; . \tag{13}$$

(Note we always keep the kinematical factors related to the electron relativistically). The central question we want to answer in this paper is, how reliable that approximation is. Clearly, this will depend on the kinematic regime. Here we shall restrict ourselves to photon energies ω and momenta $Q = \mid \vec{Q} \mid$ such that the 3N c.m. energy in the final state is essentially below the pion mass m_π:

$$E_{3N}^{c.m.} = \omega - \frac{\vec{Q}^{\,2}}{6\, m} + \epsilon_3 \leq m_\pi \tag{14}$$

(to be exact: we consider cases with $E_{3N}^{c.m.} \leq 150$ MeV) and $Q \leq 600$ MeV/c. That Q value is in fact already somewhat too high to use strictly non-relativistic kinematics and to neglect relativistic corrections in the current and the dynamics. But we consider this small excursion to be justified to acquire a first insight into a decline of FSI with increasing Q-values. Qualitatively, we do not expect a change of our results if relativistic structures will be incorporated. We shall, however, not enter into the kinematic regime with even higher Q-values and / or $E_{3N}^{c.m.}$ significantly greater than m_π.

The kinematical restriction imposed above leads to the domain D in the $Q-\omega$ plane shown in Fig. 2.

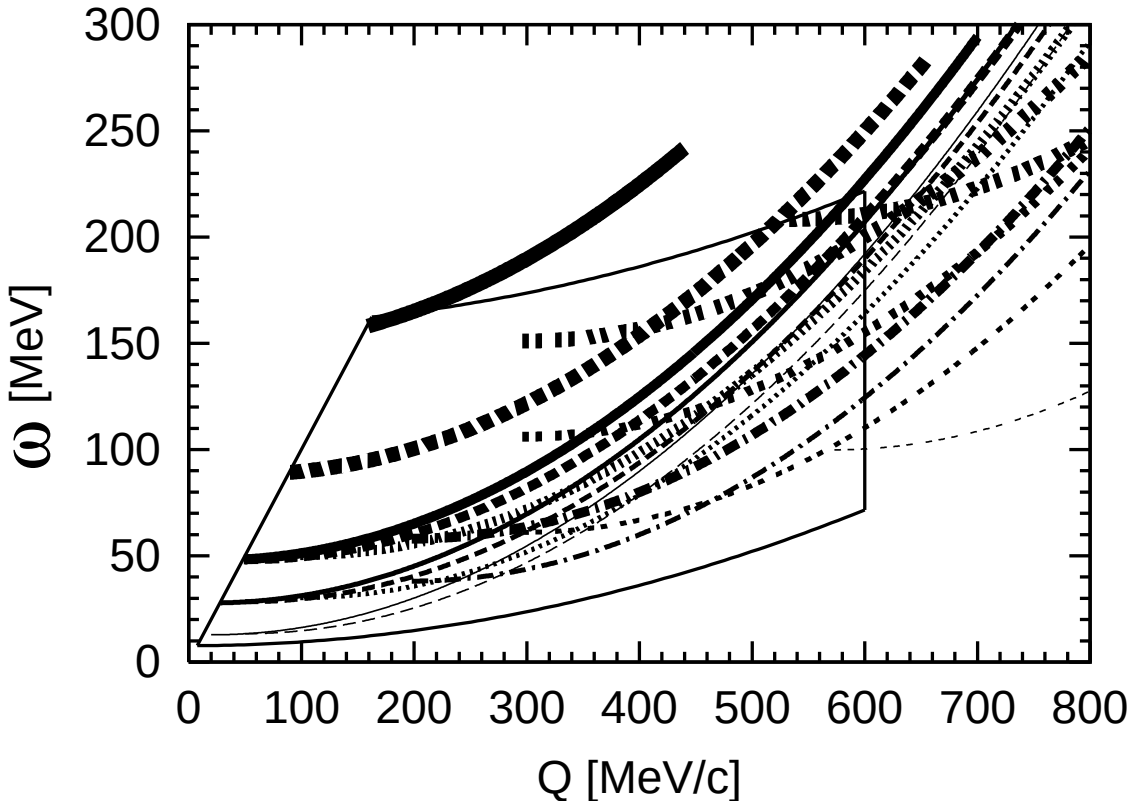

FIG. 2: The domain D in the $Q-\omega$ plane for $E_{3N}^{c.m.} \leq 150$ MeV and $Q \leq 600$ MeV/c. The additional lines correspond to fixed (k, E) values. Solid lines are for k= 0.1 fm^{-1}, dashed for k= 0.25 fm^{-1}, dotted for k= 0.5 fm^{-1}, dash-dotted for k= 1 fm^{-1}, double-dashed for k= 1.5 fm^{-1}, and triple-dashed for k= 2.7-2.9 fm^{-1}. The thickness of the lines increases with increasing E; it is minimal for E= 5 MeV and maximal for E= 140 MeV. Note that we restrict ourselves to the "less relativistic" case in Eq. (15), for which $\mid \vec{p}_1 \mid \leq \mid \vec{Q} \mid$.

Using the energy and momentum conservation in non-relativistic kinematics leads to the following connection between the variables ω, Q and k, E:

$$\omega + \epsilon_3 = \frac{(Q \pm k)^2}{2\,m} + \frac{k^2}{4\,m} + E \tag{15}$$

where in (14) and (15) ϵ_3 is the negative ^{3}He binding energy. The sign -(+) refers to $0 \leq p_1 \leq Q$ ($p_1 \geq Q$), respectively. Thus taking a pair $Q-\omega$ in D provides a relation between E and k. It is a simple matter to map the domain D into a domain D' in the $k-E$

plane. This is shown in Fig. 3 encircled by the roughly horizontal line around E= 140 MeV and the vertical line at k= 3 fm^{-1}.

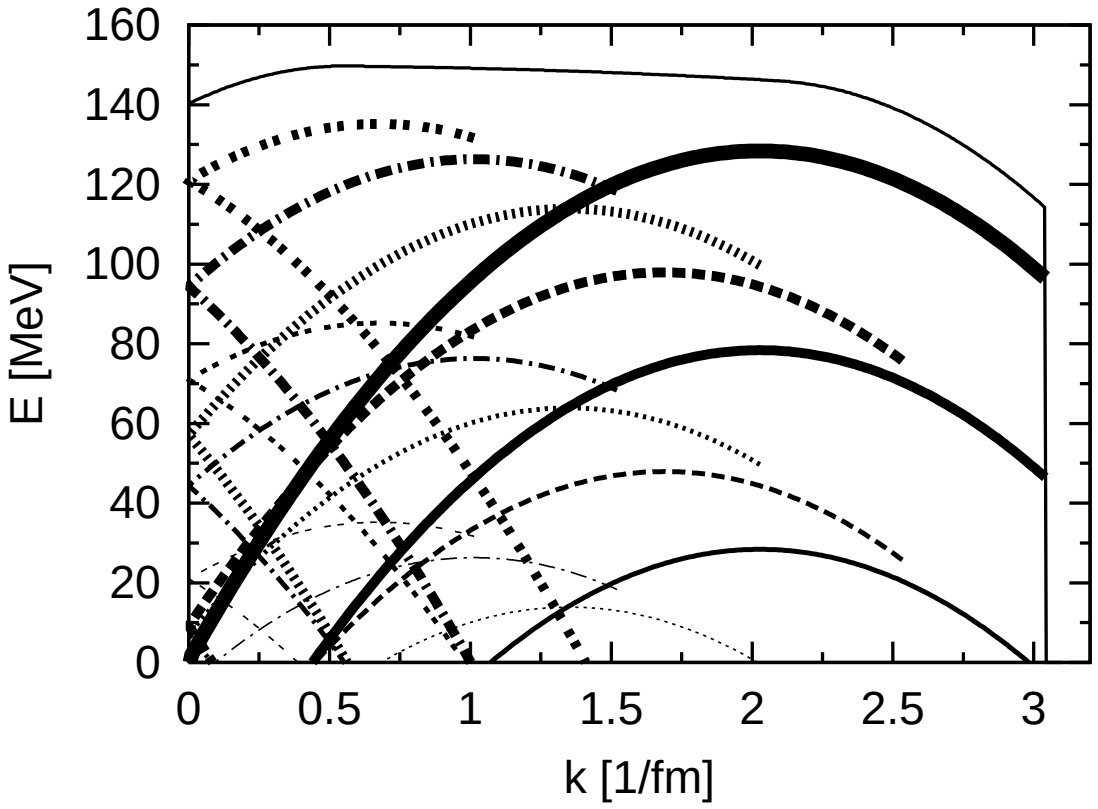

FIG. 3: The domain D' in the $k-E$ plane for $E_{3N}^{c.m.} \leq$ 150 MeV and $Q \leq$ 600 MeV/c. The solid lines correspond to Q= 600 MeV/c, dashed lines to Q= 500 MeV/c, dotted lines to Q= 400 MeV/c, dash-dotted lines to Q= 300 MeV/c, double-dotted lines to Q= 200 MeV/c. The lines thickness increases with ω: the thinest line stands for ω= 50 MeV, then the thicker and thicker lines for ω= 100, 150 and 200 MeV, respectively.

To illustrate the mappings we also display in Fig. 3 a few examples for the continuously distributed $k-E$ pairs to each fixed $Q-\omega$ out of D. We see that for fixed Q the sequence of curves shifts upwards and to the left with increasing ω. Once the bended curves hit the $k=0$ axis there appears a branch related to the sign of k in Eq. (15) reaching again to nonzero k-values. As will be clear below we are especially interested in the $Q-\omega$ pairs which lead to curves in the $k-E$ plane ending up near $E \approx 0$ and $k \approx 0$.

As is obvious from Eq. (15) that mapping from D to D' is not one-to-one.

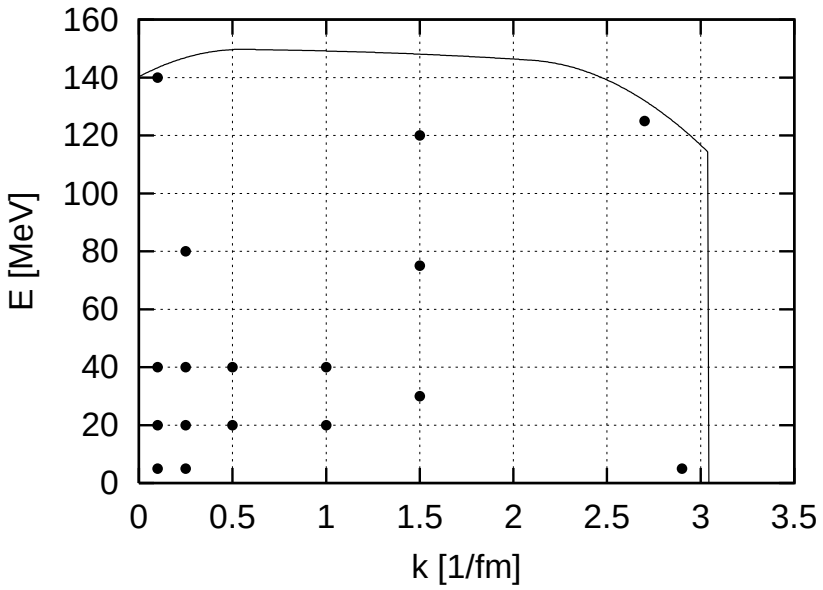

FIG. 4: The same domain D' shown in Fig. 3 in the $k-E$ plane resulting from $E_{3N}^{c.m.} \leq 150$ MeV and $Q \leq 600$ MeV/c together with (k, E) points for which the related $Q-\omega$ curves are displayed in Fig. 2. At most of those points the validity of the FSI23 approximation will be studied below. For the remaining ones the validity is not given like for others shown.

Thus, for each $k-E$ pair, only a relation between Q and ω is determined. Again quite a few examples are displayed in Fig. 2. Those $Q-\omega$ reach outside the domain D, where a relativistic treatment is obligatory and therefore outside the scope of this paper. For a better orientation of the reader, we show the chosen $k-E$ pairs in Fig. 4.

In order to investigate the usefulness of S one can use Eq.(10) and replace the response functions R_L, R_T evaluated under the simplifying assumption FSI23 by the full response functions taking FSI completely into account. This is required for the cross section given in Eq. (1). Let us call the resulting expressions $S_L(Full)$ and $S_T(Full)$, respectively. It is also of interest to neglect any FSI but keep all three terms in row 1 of Fig. 1. This we call the symmetrized plane wave impulse approximation, PWIAS, since then antisymmetrization is fully taken into account, and the resulting quantities will be denoted as $S_L(PWIAS)$ and $S_T(PWIAS)$. Finally, one can assume only the very first process in Fig. 1 to be present, leading to $S_L(PWIA)$ and $S_T(PWIA)$. In this manner we can compare $S(k, E)$ to the other three choices of dynamical input. Each $k-E$ pair fixes according to Eq. (15) ω if Q is given. Thus we shall plot the four S's for fixed (k, E) as a function of Q; in other words

as a function of the electron kinematics. By construction $S_L(PWIA)$, $S_T(PWIA)$ and S are functions of k and E only and do not depend on Q. This, however, does not hold for $S_L(PWIAS)$ and $S_T(PWIAS)$ and the results based on full treatment of FSI, $S_L(Full)$ and $S_T(Full)$.

Obviously Eq. (15) can also be written as

$$\omega + \epsilon_3 \;=\; E_1 \;+\; \frac{k^2}{4\,m} \;+\; E \tag{16}$$

with $E_1 = \frac{p_1^2}{2m}$. Therefore E_1 can be equally used as the abscissa. Note, however, that the different $E_1{}'s$ belong to different electron kinematics. This is one way to represent our results starting from fixed (k, E) values. We shall also provide examples using a fixed electron kinematics and plot the results as a function of E_1, which is more natural in relation to the experiment.

III. RESULTS

In all calculations the AV18 nucleon-nucleon potential [20] has been used without its electromagnetic parts. It is plausible to assume for the parallel kinematics considered in the paper that meson exchange currents (MEC) do not play any essential role. Thus we concentrate on the FSI effects and neglect any contribution from MEC.

Under the simplifying assumptions represented by the two encircled diagrams in Fig. 1, the response functions R_L and R_T are directly linked to the spectral function S, as shown in Eq. (10). In order to achieve insight under which conditions this form has validity, we shall cover the domain D' in Fig. 3 by a representative grid of (k, E) points chosen in Fig. 2 and marked by dots in Fig. 4.

To each such pair corresponds a quadratic relation between the photon energy ω and its three-momentum Q, as given in Eq. (15). This traces out a curve and examples thereof are shown in Fig. 2. We shall now choose those curves inside the domain D and compare the spectral function S to the expressions $S_L(Full)$ and $S_T(Full)$ evaluated under the full sequence of rescattering processes, and further compare S to $S_L(PWIAS)$ and $S_T(PWIAS)$ taking the correct antisymmetrization into account but neglecting any final state interaction and finally we compare S to $S_L(PWIA)$ and $S_T(PWIA)$ keeping only the very first process in Fig. 1. The results are displayed in Figs. 5–17.

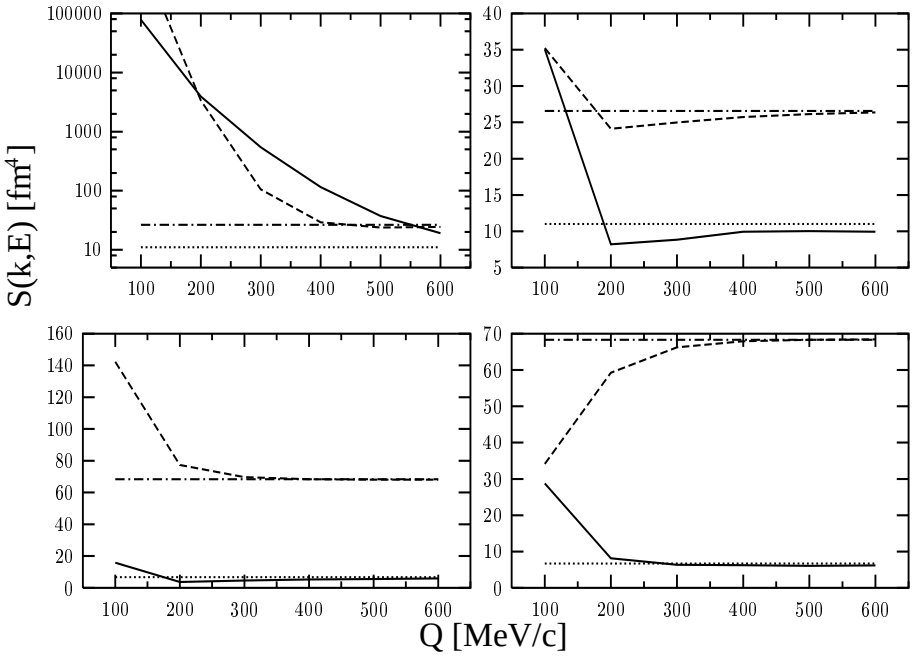

FIG. 5: The spectral function $S(k, E)$ and results based on the form given in Eq. (10) but using different dynamical assumptions for the response functions R_L and R_T as a function of the momentum transfer Q for a fixed (k, E) pair: k= 0.1 fm^{-1}, E= 5 MeV. Top figures describe the neutron knockout and bottom ones the proton case. The longitudinal (left figures) and transverse (right figures) response functions are employed. PWIA (dash-dotted line), PWIAS (dashed) and Full results (solid line) are shown. The FSI23 result (dotted) is the spectral function $S(k, E)$, which is independent of Q.

Let us first concentrate on the full calculation represented by a solid line in comparison to the spectral function S given as a dotted line in case of the proton knockout process (lower panels). We see that only for the $k - E$ pairs (0.1 fm^{-1}, 5 MeV), (0.25 fm^{-1}, 5 MeV), (0.25 fm^{-1}, 20 MeV), (0.5 fm^{-1}, 20 MeV) and (0.5 fm^{-1}, 40 MeV) chosen in Fig. 4, the two curves approach each other with increasing Q-values within the considered range of Q-values.

Though the cases (k=0.1 fm^{-1}, E=20 MeV), (k=0.1 fm^{-1}, E=40 MeV) and (k=0.25 fm^{-1}, E=40 MeV) also are small nearby pairs, the two curves do not approach each other. We have no explanation for that unexpected behavior. This means that one should stay on the safe side and better check even if both k and E approach small values whether the FSI of the knocked out nucleon is really negligible.

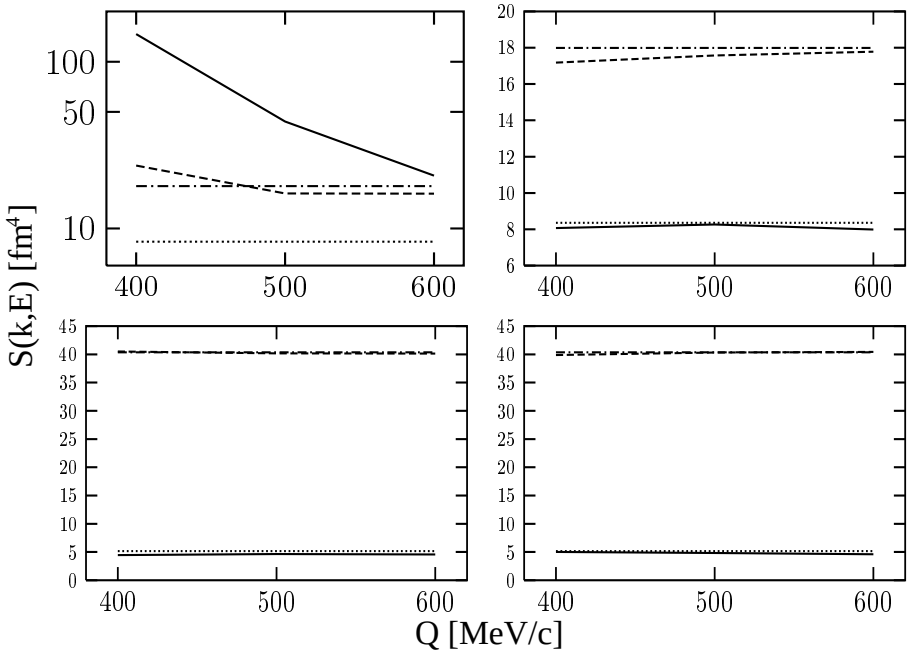

FIG. 6: The same as in Fig. 5 for k= 0.25 fm^{-1}, E= 5 MeV.

That approach is qualitatively similar for R_L and R_T. For the other $k-E$ pairs the FSI23 approximation leading to the spectral function is by far not sufficient and the full rescattering takes place. We also show the very first process in Fig. 1 denoted by PWIA and a second case where the correct antisymmetrization is kept but no rescattering process is allowed. This we denote by PWIAS. Figures 5-17 exhibit different situations in relation of the PWIAS versus the PWIA results and the PWIA versus the FSI23 results. In nearly all cases shown symmetrization in plane wave approximation (PWIAS) is quite unimportant except sometimes at the small Q-values. In the cases (1.5 fm^{-1}, 75 MeV) and (2.7 fm^{-1}, 125 MeV) symmetrization, however, is quite important. All that is easily understood regarding the momentum values for the two additional processes of PWIAS. In the case of PWIA the ^{3}He wave function $\Psi_{^3\mathrm{He}}(\vec{p},\vec{q})$ is evaluated for $\vec{p}=\frac{1}{2}\left(\vec{p}_2-\vec{p}_3\right)$ and $\vec{q}=\vec{p}_1-\vec{Q}$. For the two additional processes present in PWIAS the corresponding arguments are $\left(\vec{p}=\frac{1}{2}\left(\vec{p}_1-\vec{p}_2\right),\vec{q}=\vec{p}_3-\vec{Q}\right)$ and $\left(\vec{p}=\frac{1}{2}\left(\vec{p}_3-\vec{p}_1\right),\vec{q}=\vec{p}_2-\vec{Q}\right)$. Interestingly in case of Figs. 16 and 17 the PWIA and FSI23 results agree very well. Thus the final state interaction among the two spectator nucleons is negligible. If additionally the symmetrization and all of the final state interaction were negligible, one would have a perfect view right away into the ^{3}He wave function, since S

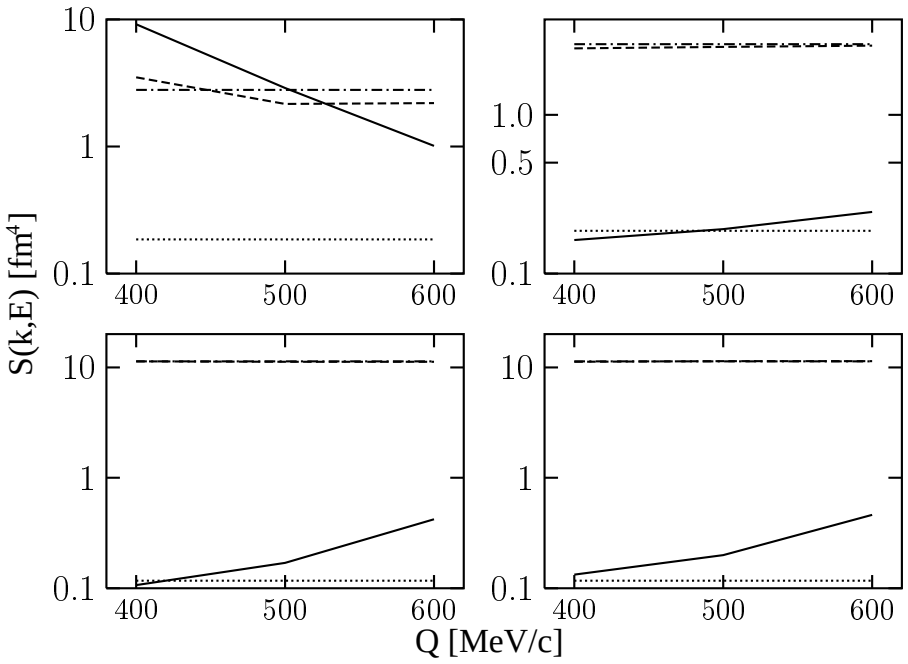

FIG. 7: The same as in Fig. 5 for k= 0.1 fm^{-1}, E= 20 MeV.

evaluated under PWIA condition displays directly the magnitude of the ^{3}He wave function. (This is obvious from Eq. (7) if one drops the contribution proportional to $t_{23}G_0$). That neglection is, however, not justified as documented in Figs. 16 and 17. Already the correct antisymmetrization, which is independent of FSI changes the results totally.

In [13] $S(k, E)$ is displayed together with S evaluated under the PWIA condition. They essentially agree for $k \geq 1.5$ fm^{-1} along $E = k^2/(4m)$. As examples one could take $k =$ 2 fm^{-1} corresponding to $E \approx 40$ MeV or $k = 3$ fm^{-1} with E about 90 MeV. This suggested direct insight into the ^{3}He wave function. In view of our results shown in Figs. 16 and 17 this suggestion is not valid if the electron kinematics belongs to the domain D.

This does, of course, not exclude that outside of D the situation might be more favorable to such an ideal situation. In Fig. 2 one can see that for those pairs of $k - E$ values there are continuous $\omega - Q$ pairs, where such an ideal situation might exist. This requires, however, above all a relativistic treatment and taking all the additional dynamical ingredients into account, which is outside the scope of the present study. Please also note that for c.m. 3N energies above the pion threshold no nuclear forces comparable in quality to the ones below are available.

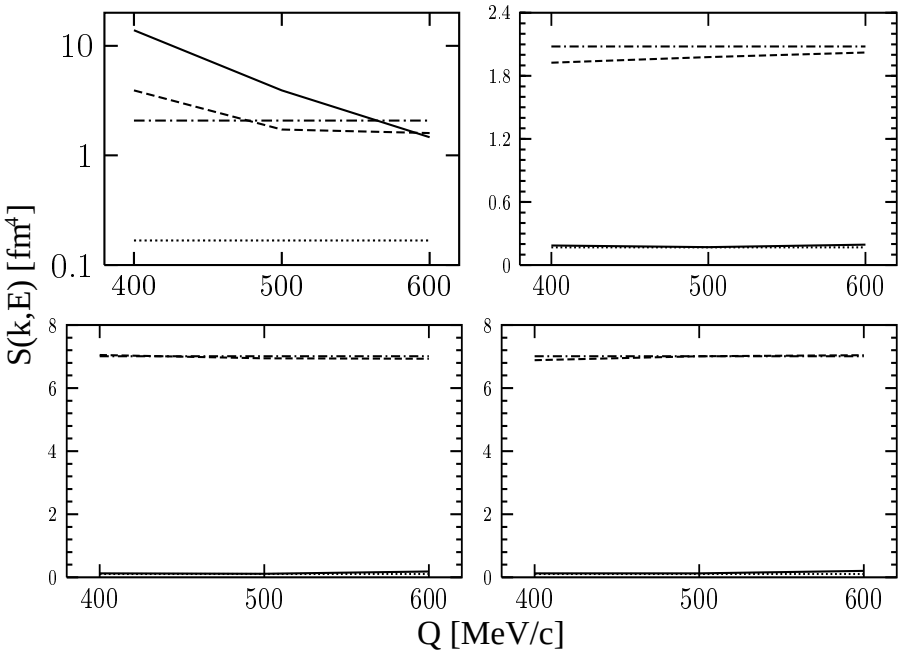

FIG. 8: The same as in Fig. 4 for k= 0.25 fm^{-1}, E= 20 MeV.

Regarding now the neutron knockout even at low $k-E$ values the spectral function in case of R_L is insufficient. For R_T, however, the situation is quite similar to the proton knockout. Thus neutron knockout for ^{3}He without separation of R_L and R_T is not suitable for that application of the spectral function S.

We have to conclude that for most of the $Q-\omega$ values in the domain D the use of the spectral function is quantitatively not justified and identifying experimentally extracted S-functions after integration over E with the ^{3}He momentum distribution is not correct. It is only for a certain group of very small $k-E$ values (both) and for proton knockout that $S_L(Full)$ and $S_T(Full)$ approach S at the higher Q values in the domain D.

It is at least that "corner" of the $k-E$ domain where the theoretical prediction should be valid since only the NN t-matrix together with the ^{3}He wave function enter at low momenta. Therefore precise data there would be quite important to validate at least that expectation. For other regions inside D the full dynamics is acting.

In actual experiments it is natural to present the data for the process ^{3}He$(e,e'N)$ for a given $Q-\omega$ pair as a function of E_1, the energy of the knocked out nucleon. In this case the $k-E$ values trace out a curve in the domain D' as shown in Fig. 3. Of course investigating

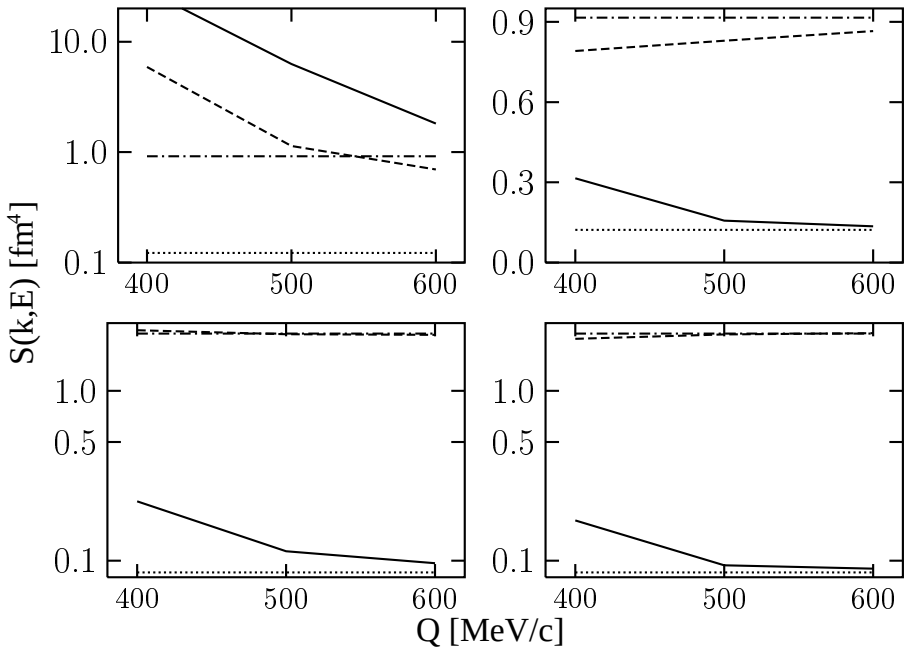

FIG. 9: The same as in Fig. 5 for k= 0.5 fm^{-1}, E= 20 MeV.

such a scenario there will be no new information beyond the one we already displayed. Nevertheless since this is what appears naturally in an experiment we would like to show the corresponding S-curves now as a function of E_1. First we choose proton knockout and take $Q-\omega$ values which in the $k-E$ plane lead to curves ending up in the "corner", where both k and E are rather small. As seen from Eq. (15) and displayed in some examples in Fig. 3 suitable cases are: $\omega = 100$ MeV, $Q = 400$ MeV/c; $\omega = 100$ MeV, $Q = 500$ MeV/c; $\omega = 150$ MeV, $Q = 600$ MeV/c.

In all these cases k and E get very small when E_1 approaches its maximal value. This is illustrated in Figs. 18–20. We restrict ourselves to the upper end of the energy E_1 since only there S and $S(Full)$ approach each other.

We see a very nice coincidence of S with the full results at the upper end of E_1, both for R_L and R_T. Thus the full cross section can be rather well represented by the spectral function approximation.

As counterexamples one can choose: $\omega = 100$ MeV, $Q = 200$ MeV/c; $\omega = 200$ MeV, $Q = 300$ MeV/c shown in Figs. 21–22. We see indeed, that there is no agreement of S with the full results, neither in relation to R_L nor to R_T and the approximation using S is not

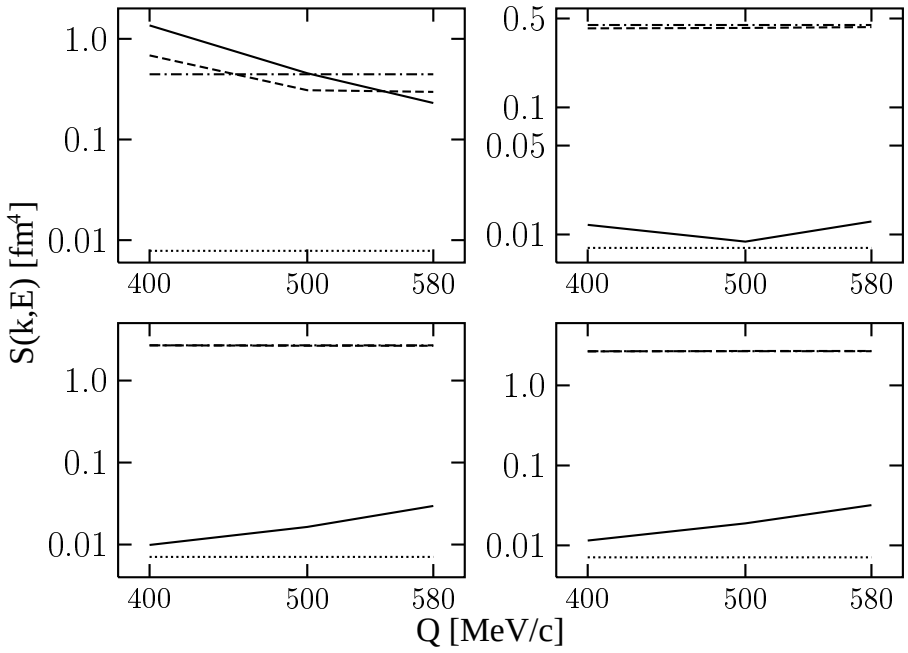

FIG. 10: The same as in Fig. 5 for k= 0.1 fm^{-1}, E= 40 MeV.

acceptable.

In the case of neutron knockout only R_T can be approximated by the spectral function and therefore the approximation of the full cross section is not suitable. We show in Figs. 23–24 only two examples, for ω= 100 MeV, Q= 500 MeV/c and ω= 150 MeV, Q= 600 MeV/c.

Finally one example is displayed in Fig. 25 for ω= 100 MeV and Q= 200 MeV/c, where the spectral function even for R_T is not a sensible approximation.

One has to conclude that the spectral function S is not a good tool to analyze neutron knockout inside the domain D except for special $Q-\omega$ pairs at the upper end of E_1 in case of the transversal response.

Finally we would like to add a remark on the extraction of electromagnetic form factors of the nucleons. In the case that the FSI23 approximation is valid or in other words the use of the spectral function is justified, the electromagnetic form factors are directly accessible. As seen in Eq. (11) a $L-T$ separation provides direct access to both, G_E and G_M. It appears interesting to check that approach firstly in the case of the proton knockout, where the form factors are known. In the case of the neutron knockout the transverse response function R_T can be well controlled under the kinematic conditions discussed above and therefore

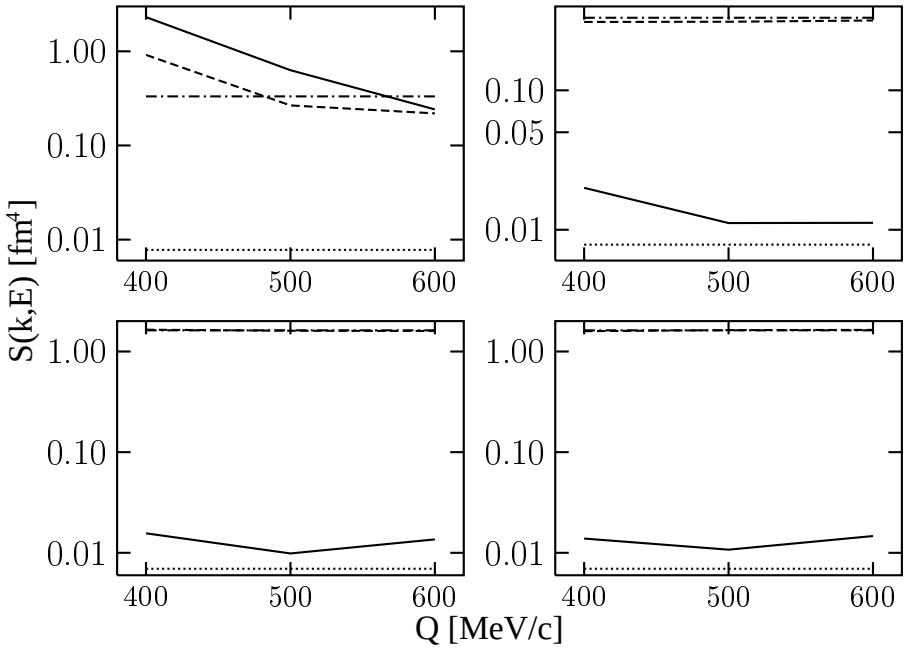

FIG. 11: The same as in Fig. 5 for k= 0.25 fm^{-1}, E= 40 MeV.

access to G_M^n appears possible. In the case of G_E^n it might also work at higher energy and momentum transfers, which are however outside the kinematic regime investigated in this study.

IV. SUMMARY

We reviewed briefly the formulation of the full treatment of the final state interaction for the process ^{3}He$(e, e'N)$ in the Faddeev scheme. We showed that the processes underlying the concept of the spectral function are just the very first two diagrams in an infinite series of diagrams caused by rescattering and complete antisymmetrization. The spectral function S is directly related to both response functions, R_L and R_T, under those simplifying assumptions. We used the same formal relation which leads to S but now working with the response functions which include the complete final state interaction. This leads to quantities $S_L(Full)$ and $S_T(Full)$, which can be compared to S. The comparison was restricted to a kinematical regime where a non-relativistic treatment appears mostly justified. Thus we restricted $E_{3N}^{c.m.}$ to be below the pion threshold, more precisely to stay below 150 MeV and the magnitude of the photon momentum $\vec{Q}$ to be below 600 MeV/c. This defined a domain

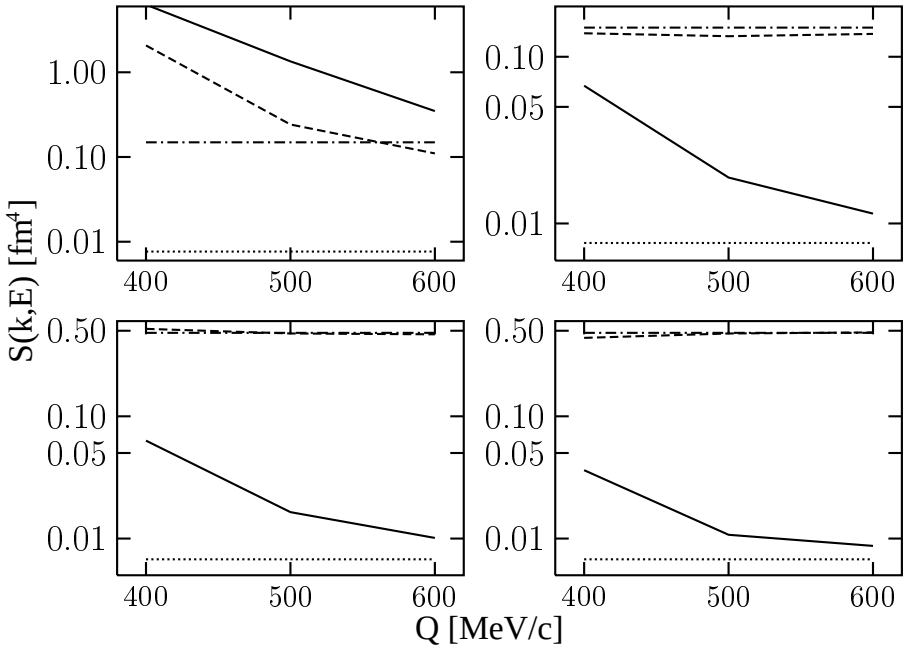

FIG. 12: The same as in Fig. 5 for k= 0.5 fm^{-1}, E= 40 MeV.

D in the $Q-\omega$ plane. The kinematical conditions for parallel knockout lead then to a quadratic equation connecting $Q-\omega$ to $k-E$, the missing momentum and missing energy. Thus the domain D is mapped into a domain D' in the $k-E$ plane and vice versa. Our results show that for proton knock out $S_L(Full)$ and $S_T(Full)$ agree with the approximate quantity S (appropriately corrected by electromagnetic form factors and kinematical factors) if both k and E are very small. Unfortunately this is not always the case and therefore the validity of that approximation has better to be checked in each case. For the rest of the domain D' in the $k-E$ plane S is not a valid approximation. Specifically there occur intriguing cases, where inside D' S coincides with the most simple approximate treatment of the process, namely pure PWIA. This suggest a direct view into the 3He wave function. However, this is quite misleading under the kinematics investigated here since even the complete antisymmetrization totally destroys that simple picture not to speak of the final state interaction of the knocked out nucleon with the other two.

In the case of neutron knockout, only R_T can be approximated by S under certain kinematical conditions (low $k-E$ values). In the case of R_L the smallness of G_E^n in relation to G_E^p leads always to an important contribution of the absorption of the photon by the two

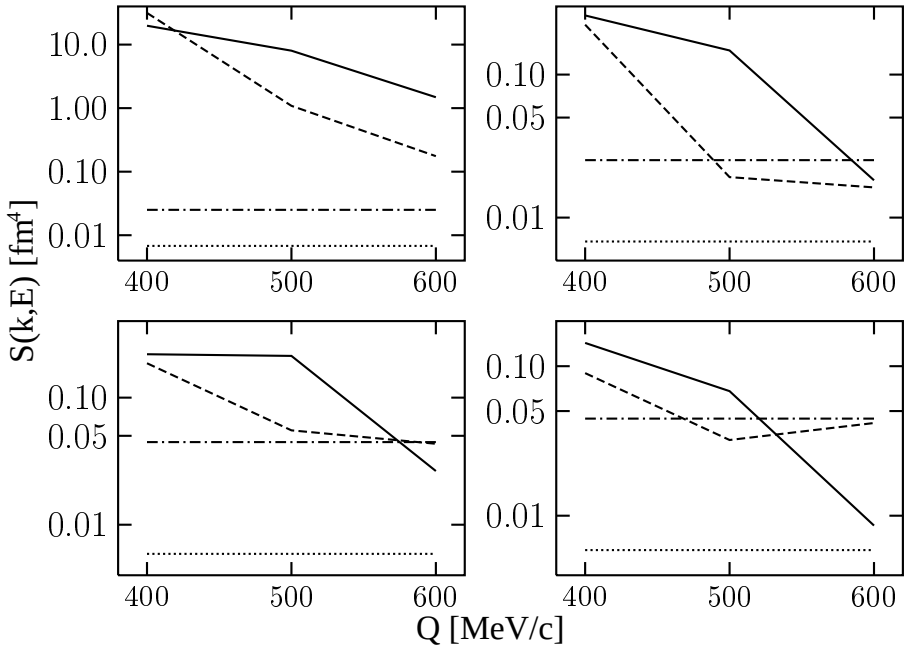

FIG. 13: The same as in Fig. 5 for k= 1.0 fm^{-1}, E= 40 MeV.

protons, which then by final state interaction knock out the neutron. So R_L in the case of neutron knockout cannot be approximated by S in the kinematic regime investigated in our study. Finally we would like to note that the concept of S might be useful to extract electromagnetic nucleon form factors if the kinematical conditions are suitable.

Acknowledgments

This work was supported by the Polish Committee for Scientific Research under grant no. 2P03B00825, by the NATO grant no. PST.CLG.978943 and by DOE under grants nos. DE-FG03-00ER41132 and DE-FC02-01ER41187. One of us (W.G.) would like to thank the Foundation for Polish Science for the financial support during his stay in Kraków. The numerical calculations have been performed on the cray SV1 and T3E of the NIC in Jülich, Germany.

[1] A.E.L. Dieperink, T. De Forest Jr., Ann. Rev. Nucl. Sci. **25**, 1 (1975).

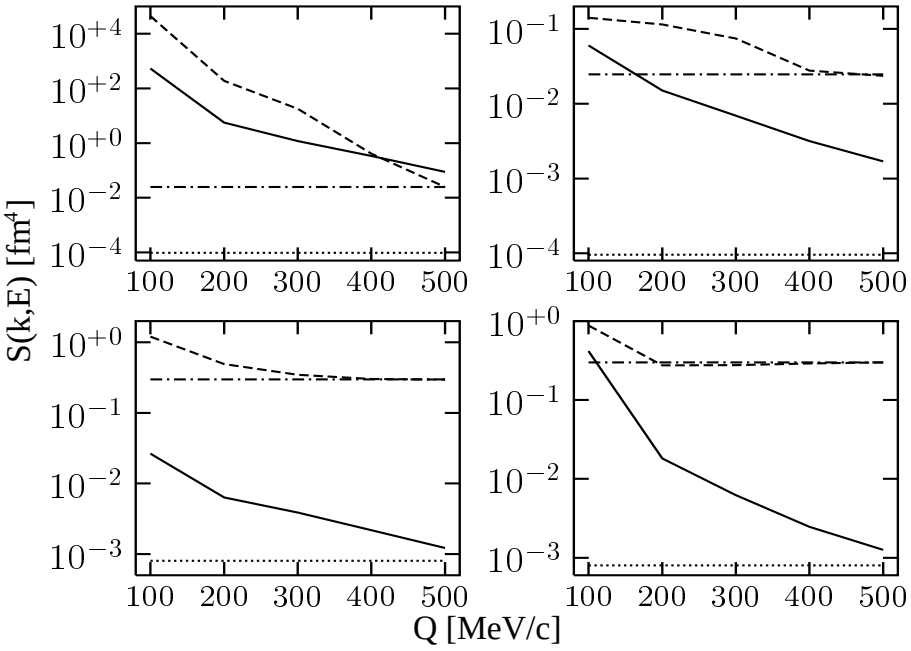

FIG. 14: The same as in Fig. 5 for k= 0.25 fm^{-1}, E= 80 MeV.

[2] A.E.L. Dieperink, T. De Forest Jr., I. Sick, R.A. Brandenburg, Phys. Lett. **63B**, 261 (1976).

[3] C. Ciofi degli Atti, E. Pace, G. Salmè, "Electrodisintegration of the few-body systems and realistic interactions", Lecture Notes in Physics **86**, 316 (1979); "Few Body Systems and Electromagnetic interactions", proceedings of the Workshop held in Frascati, Italy, March 7-10, 1978.

[4] C. Ciofi degli Atti, Progress Part. Nucl. Phys. **3**, 163 (1980).

[5] C. Ciofi degli Atti, E. Pace, G. Salmè, Phys. Rev. C**21**, 805 (1980).

[6] C. Ciofi degli Atti, E. Pace, and G. Salmè, "Nucleon momentum distribution in finite nuclei", published in the Volume "Perspectives in Nuclear Physics at Intermediate Energies", S. Boffi, C. Ciofi degli Atti nd M.M. Giannini Eds., World Scientific Publishing Co., Singapore, 1984.

[7] C. Ciofi degli Atti, E. Pace, G. Salmè, Phys. Rev. C**51**, 1108 (1995).

[8] H. Meier-Hajduk, Ch. Hajduk, P.U. Sauer, and W.Theis, "Quasi-elastic electron scattering from ^{3}He", Nucl. Phys. **A395**, 332 (1983).

[9] R.-W. Schulze and P.U. Sauer, Phys. Rev. C**48**, 38 (1993).

[10] P.U. Sauer and R.-W. Schulze, "Spin-dependent inelastic electron scattering from three-nucleon bound states", in "Contemporary Topics in Medium Energy Physics", Eds. K. Goeke

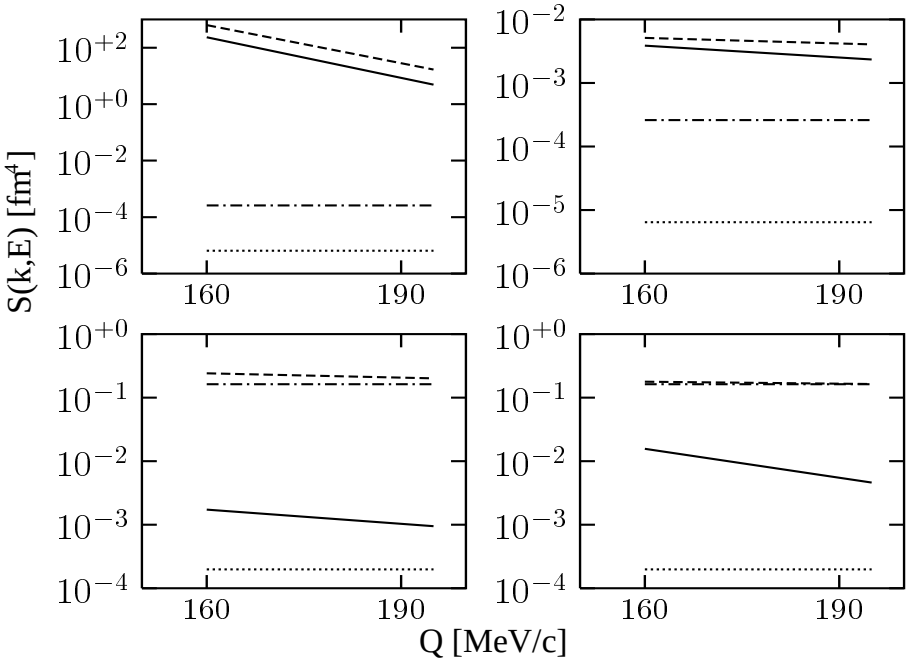

FIG. 15: The same as in Fig. 5 for k= 0.1 fm^{-1}, E= 140 MeV.

et al., Plenum Press, New York, 1994.

[11] S. Boffi, C. Giusti, F.D. Pacati, M.Radici, *Electromagnetic Response of Atomic Nuclei*, Clarendon Press, Oxford, 1996.

[12] A.Kievsky, E. Pace, G. Salmè, and M. Viviani, Phys. Rev. C**56**, 64 (1997).

[13] C. Ciofi degli Atti and L.P. Kaptari, Phys. Rev. C**66**, 044004 (2002).

[14] C. Ciofi degli Atti and L.P. Kaptari, Nucl. Phys. **A699**, 49c (2002).

[15] J. Golak, H. Kamada, H. Witała, W. Glöckle, and S. Ishikawa, Phys. Rev. C**51**, 1638 (1995); J. Golak, H. Witała, H. Kamada, D. Hüber, S. Ishikawa, and W. Glöckle, Phys. Rev. **C 52**, 1216 (1995); S. Ishikawa, J. Golak, H. Witała, H. Kamada, W. Glöckle, D. Hüber, Phys. Rev. C**57**, 39 (1998); J. Golak, G. Ziemer, H. Kamada, H. Witała, and W. Glöckle, Phys. Rev. C**51**, 034006 (2001).

[16] T. W. Donnelly, A. S. Raskin, Ann. Phys. (N.Y.) **169**, 247 (1986).

[17] A.S. Raskin and T.W. Donnelly, Ann. Phys. (N.Y.) **191**, 78 (1989).

[18] R. Skibiński *et al.*, Phys. Rev. C**67**, 054001 (2003).

[19] W. Glöckle, *The Quantum Mechanical Few-Body Problem*, Springer-Verlag, Berlin, 1983.

[20] R. B. Wiringa, V. G. J. Stoks, R. Schiavilla, Phys. Rev. **C51**, 38 (1995).

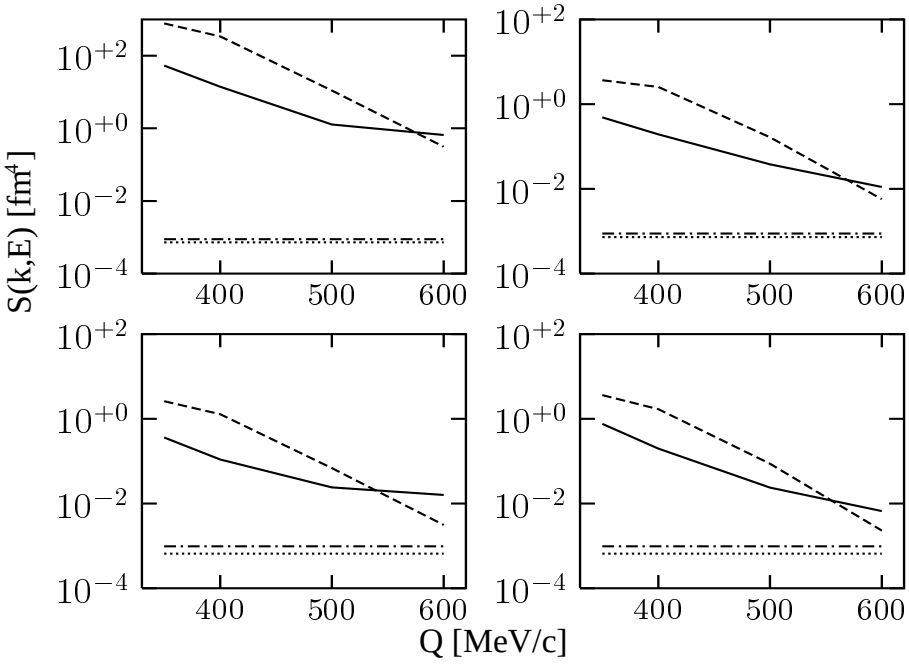

FIG. 16: The same as in Fig. 5 for k= 1.5 fm^{-1}, E= 75 MeV.

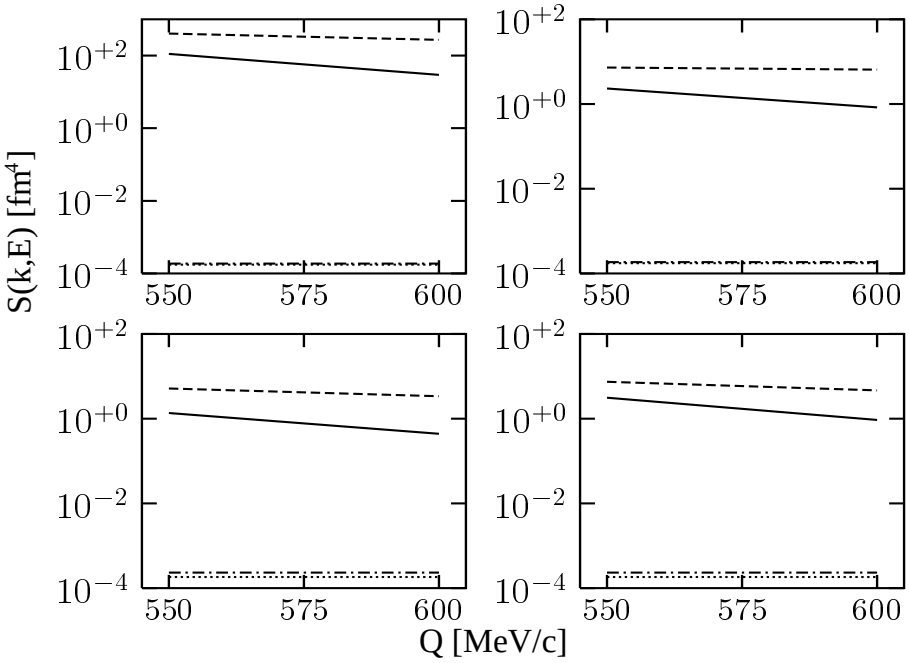

FIG. 17: The same as in Fig. 5 for k= 2.7 fm^{-1}, E= 125 MeV.

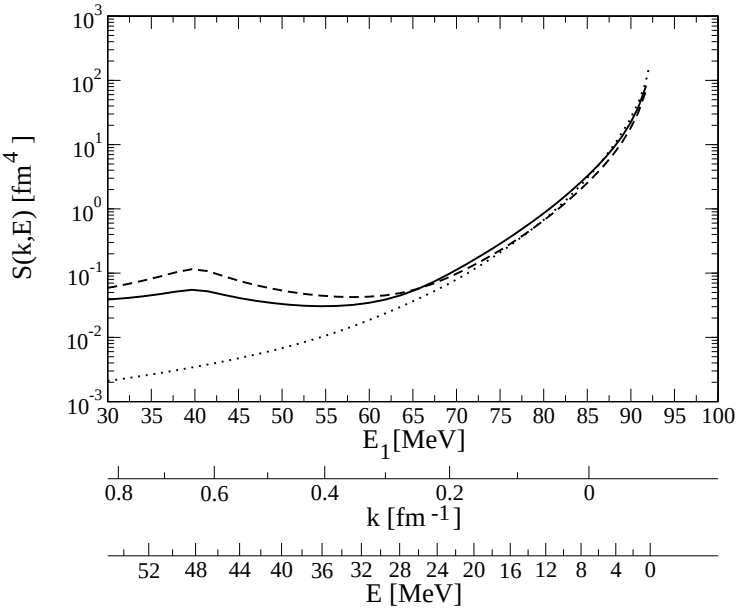

FIG. 18: The spectral function $S(k, E)$ for the proton knockout (dotted line), Full results based on the form given in Eq. (10) for the response functions R_L (dashed line) and Full results for the response functions R_T (solid line) for a fixed $(Q - \omega)$ pair: ω= 100 MeV, Q= 400 MeV/c as a function of the ejected proton energy E_1 for the parallel kinematics $\vec{p}_1 \parallel \vec{Q}$. The corresponding values of k and E are also indicated.

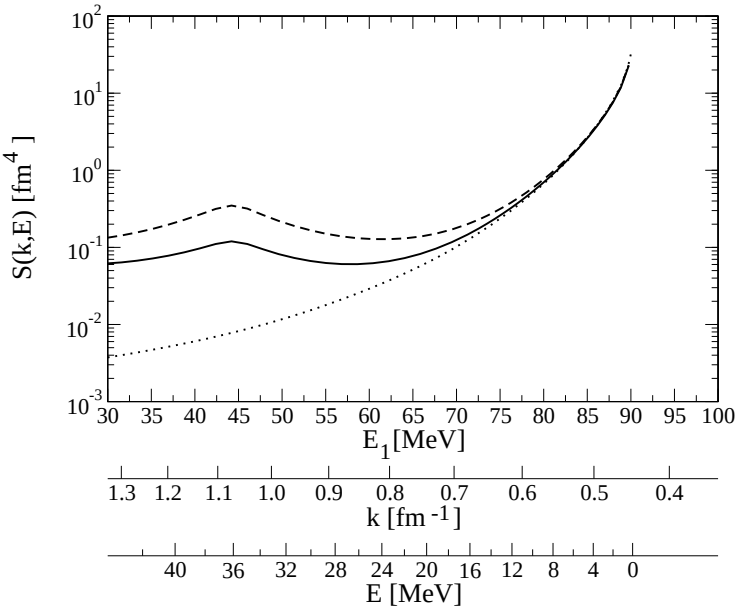

FIG. 19: The same as in Fig. 18 for ω= 100 MeV and Q= 500 MeV/c.

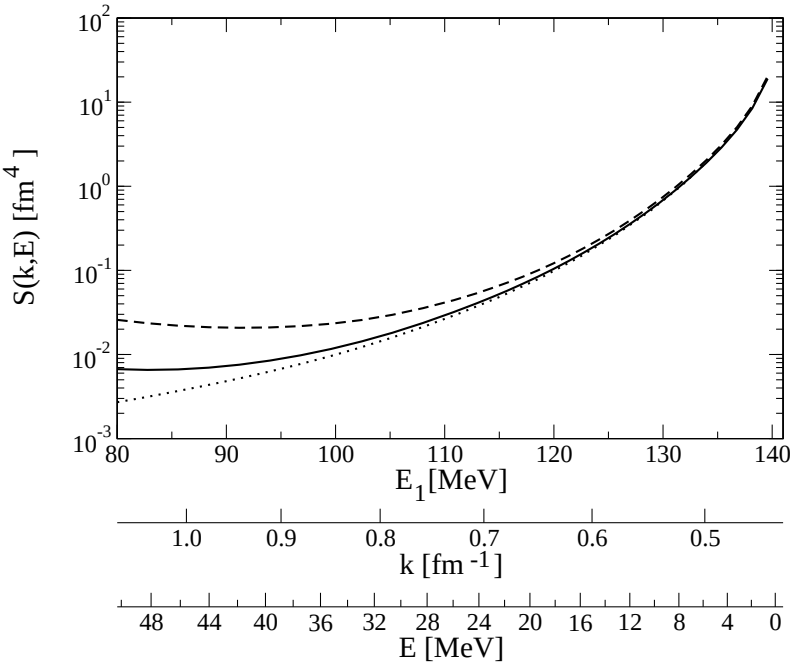

FIG. 20: The same as in Fig. 18 for ω= 150 MeV and Q= 600 MeV/c.

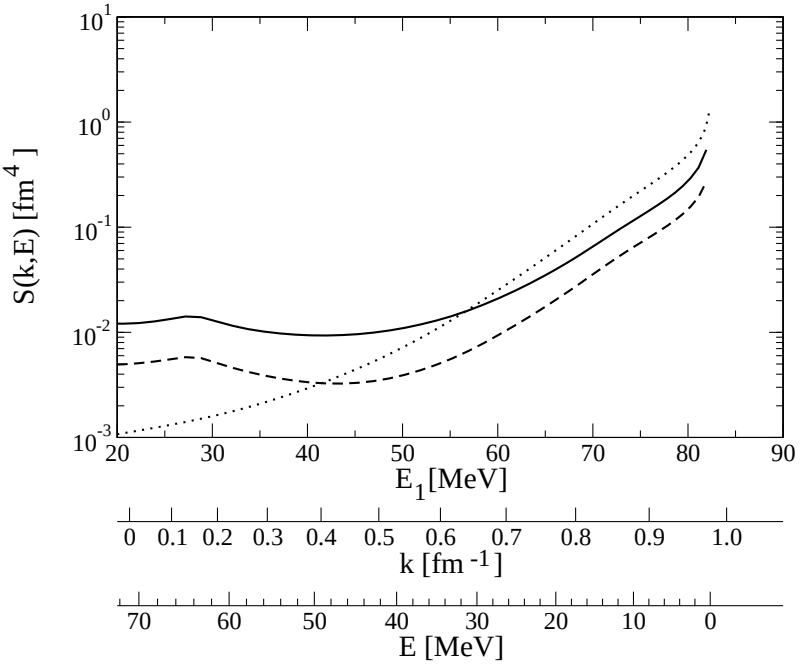

FIG. 21: The same as in Fig. 18 for ω= 100 MeV and Q= 200 MeV/c.

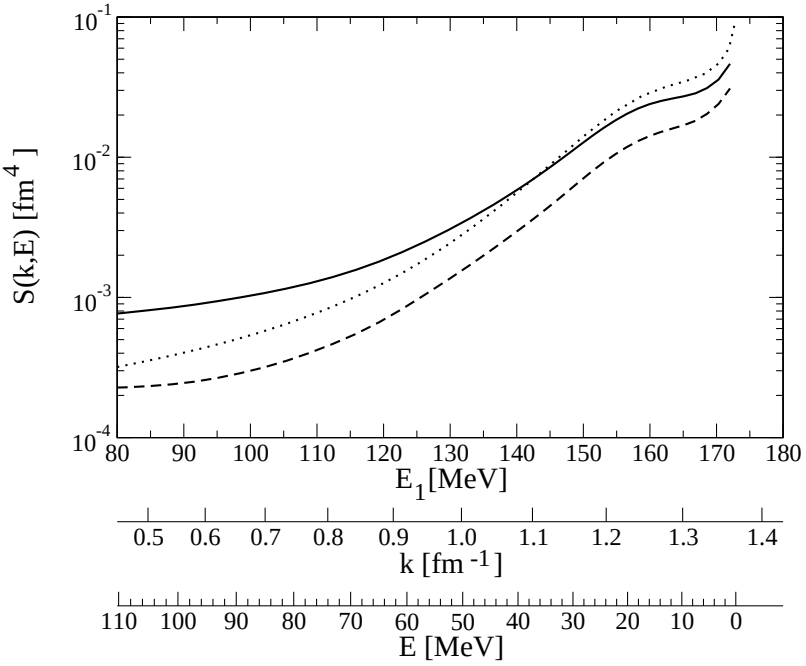

FIG. 22: The same as in Fig. 18 for ω= 200 MeV and Q= 300 MeV/c.

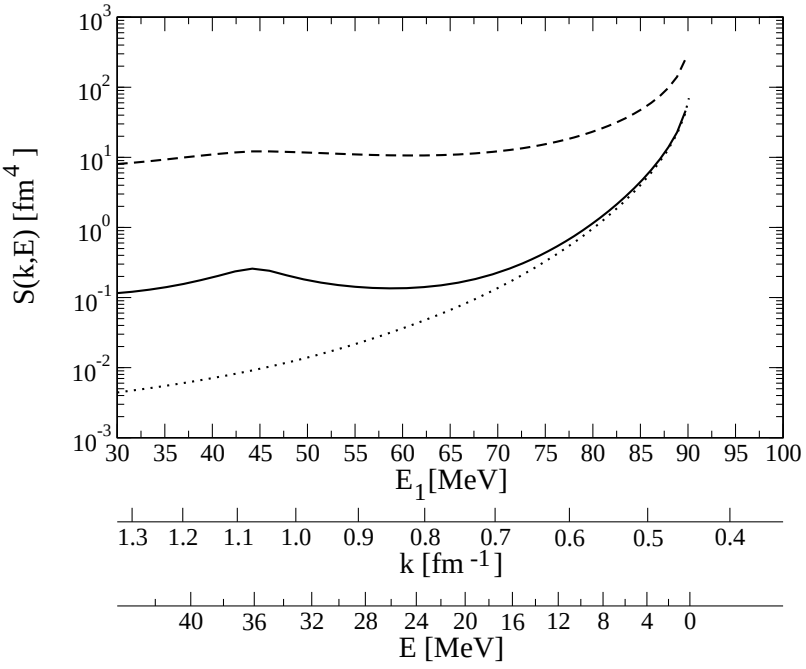

FIG. 23: The same as in Fig. 19 for the neutron knockout.

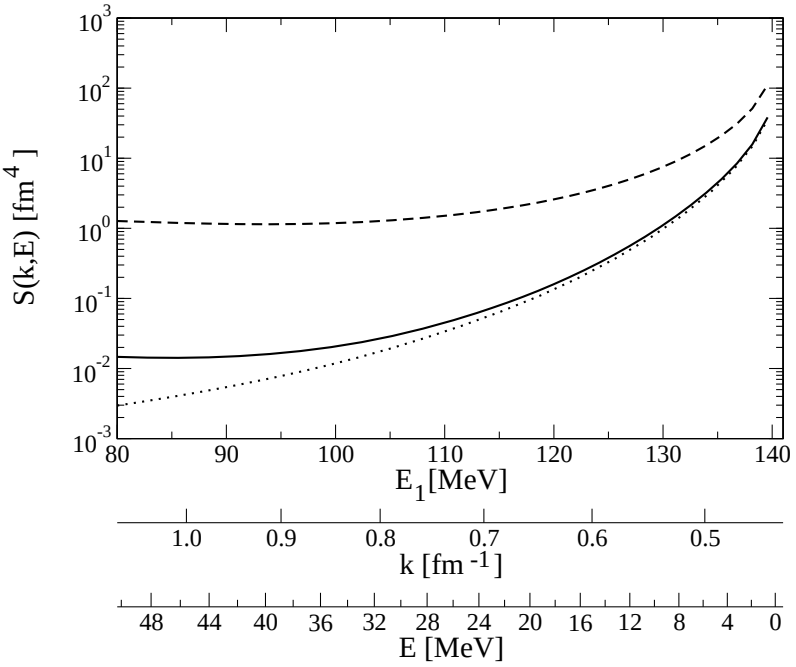

FIG. 24: The same as in Fig. 20 for the neutron knockout.

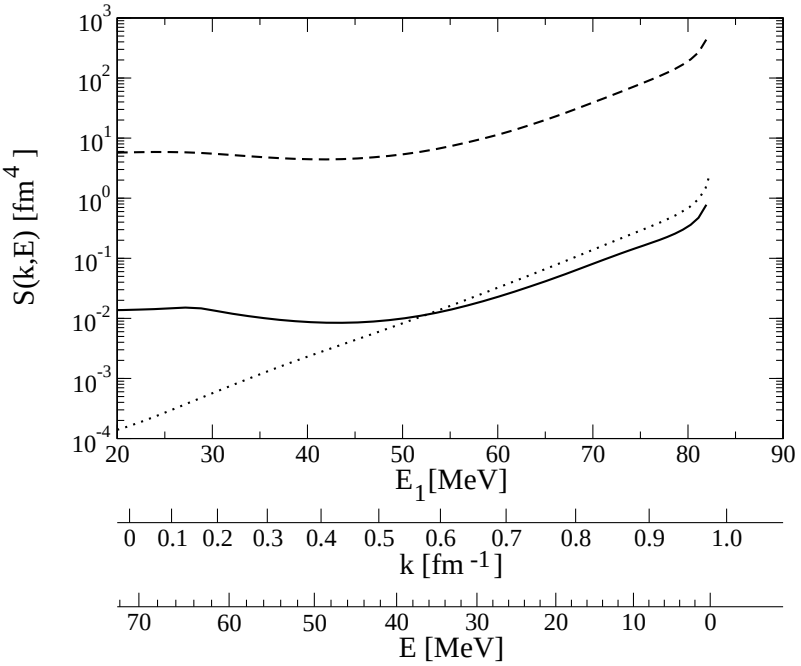

FIG. 25: The same as in Fig. 24 for the neutron knockout and ω= 100 MeV, Q= 200 MeV/c.